



# Attribution of the impact of the February 2018 sudden stratospheric warming on mortality in the Nordics and United Kingdom

Philip Rupp<sup>1</sup>, Liliana Vázquez Fernández<sup>2,3</sup>, William J. M. Seviour<sup>4</sup>, and Thomas Birner<sup>1,5</sup>

Correspondence: Philip Rupp (philip.rupp@lmu.de) and William Seviour (W.Seviour@exeter.ac.uk)

Abstract. Sudden stratospheric warming (SSW) events can trigger extended periods of cold surface weather in Europe, with potential consequences for public health. While previous work has established statistical links between SSWs and increased winter mortality, quantitative attribution of deaths to specific SSW events remains limited, particularly across different regions and data resolutions. This study presents a framework that combines exposure-response curves with stratospherically nudged ensemble forecasts to robustly attribute excess mortality to the February 2018 SSW event and its associated cold surface anomalies. We analyse mortality in various UK regions as well as three Nordic countries using a combination of daily, weekly and monthly aggregated mortality datasets. Exposure-response curves are derived using both distributed lag nonlinear models (DLNMs) and a simpler binning-based approach, allowing evaluation across varying temporal resolutions and data constraints. We find that while the Nordic countries experienced the strongest post-SSW temperature anomalies, the highest attributable mortality risk impacts occurred in the UK. This is explained by the steepness of the cold branch of the exposure-response relationship in southern UK regions, likely reflecting lower population-level adaptation to cold weather. Our results suggest that approximately 750 deaths in England and Wales and 250 in the Nordic countries can be attributed to the 2018 SSW. We show that even with coarser temporal resolution data, the binning-based approach yields consistent mortality estimates, supporting its use in data-limited settings. The regional variation in exposure-response characteristics further highlights the need to consider both meteorological hazard magnitude and societal vulnerability. Beyond mortality, the framework is applicable to other societal impacts of extreme weather, providing a flexible and interpretable tool for retrospective attribution and climate risk assessment.

Keywords. Sudden stratospheric warming, health impact, mortality, cold spells

#### 1 Introduction

Severe weather events involving temperature extremes pose significant public health challenges. A substantial focus of existing literature lies on health impacts of heat extremes, while the total amount of excess deaths attributable to cold anomalies can be several times higher (Gasparrini et al., 2015). This is because even moderate drops in temperature can sharply elevate health

<sup>&</sup>lt;sup>1</sup>Meteorological Institute Munich, Ludwig Maximilian University of Munich, Munich, Germany

<sup>&</sup>lt;sup>2</sup>Division for Climate and Environmental Health, Norwegian Institute of Public Health, Oslo, Norway

<sup>&</sup>lt;sup>3</sup>Department of Biostatistics, Institute of Basic Medical Sciences, University of Oslo, Oslo, Norway

<sup>&</sup>lt;sup>4</sup>Department of Mathematics and Statistics and Global Systems Institute, University of Exeter, Exeter, UK

<sup>&</sup>lt;sup>5</sup>Division for Climate and Environmental Health, Norwegian Institute of Public Health, Oslo, Norway



30

50



risks (e.g., Analitis et al., 2008; Sarofim et al., 2016; Walkowiak et al., 2024). For instance, a study by Zeka et al. (2014) has shown that a 1 K decrease in winter maximum temperature in Ireland can correspond to about a 6.4% increase in all-cause mortality. However, epidemiological research indicates substantial regional difference in the impacts of temperature anomalies on mortality risk, depending on the general adaptation to cold due to climatological temperature values, socio-economic factors like access to adequate heating or demographic differences (Group, 1997; Kysely et al., 2009; Hajat et al., 2014; Mistry et al., 2022). Correspondingly, predicting the actual impacts of weather and climate anomalies has thus become a topic of increasing interest to allow for more effective public health planning and targeted mitigation measures (Lowe et al., 2015; Pyrina et al., 2025).

A key phenomenon that has been linked to prolonged periods of increased risk of cold extremes in Europe are sudden stratospheric warming (SSW) events (Kolstad et al., 2010; Kretschmer et al., 2018; Huang et al., 2021). These events involve a rapid increase in polar stratospheric temperatures and a disruption of the stratospheric polar vortex (see review by Baldwin et al., 2021). Despite being located in the stratosphere, the associated circulation anomalies can propagate downward to the surface and affect tropospheric weather patterns (Baldwin and Dunkerton, 2001). The tropospheric response to SSWs typically includes a tendency for negative phases of large-scale circulation patterns like the Arctic Oscillation (AO) or the North Atlantic Oscillation (NAO). These circulation anomalies then often lead to colder-than-average conditions and an increased likelihood for cold spells across Eurasia, including Northern Europe and the United Kingdom. Due to the generally long time scales of the stratosphere (Baldwin et al., 2003), the surface impacts can last for several weeks to months (also referred to as subseasonal time scales) and hence SSWs offer unique opportunities for improved forecasts (Kautz et al., 2020; Domeisen et al., 2020; Büeler et al., 2021; Spaeth et al., 2024).

The February 2018 SSW is an excellent example: this event has been shown to be associated with severe cold conditions and anomalous snowfall across Northern Europe and the UK, widely termed the 'Beast from the East' (Greening and Hodgson, 2019; King et al., 2019; Overland et al., 2020). In the present study we use this 2018 event as case study, to attribute potential excess mortality to the occurrence of an SSW. Figure 1 shows the surface temperature anomaly following the 2018 event and the composite mean over many SSWs for the United Kingdom and the Nordic countries Norway, Sweden and Finland (see Section 2 for details of the data and SSW dates used). It can be seen that the surface temperature response, while overall negative and robust, shows clear spatial patterns. In particular, northern Europe typically shows substantially stronger temperature anomalies compared to, e.g., the United Kingdom.

Recent studies directly link SSW-induced cold spells to significant mortality increases. For instance, analyses of UK mortality following major SSW events reveal approximately 620 excess deaths attributable to these events, on average (Charlton-Perez et al., 2021). Such findings underscore the tangible public health consequences of stratospheric variability. Yet, quantitative assessments of mortality impacts related explicitly to SSW events remain limited, particularly in terms of regional differences of these impacts. This geographical knowledge gap, in addition to the long-leadtime forecasting potential of SSW events, motivates the need for broader regional assessments of the socio-economic impacts of SSWs to enhance targeted preparedness.

Quantifying cold-related health impacts typically relies on statistical models linking an exposure variable (like temperature) and a response variable (like mortality), e.g., via exposure–response curves (Huang et al., 2012; Gasparrini and Armstrong,





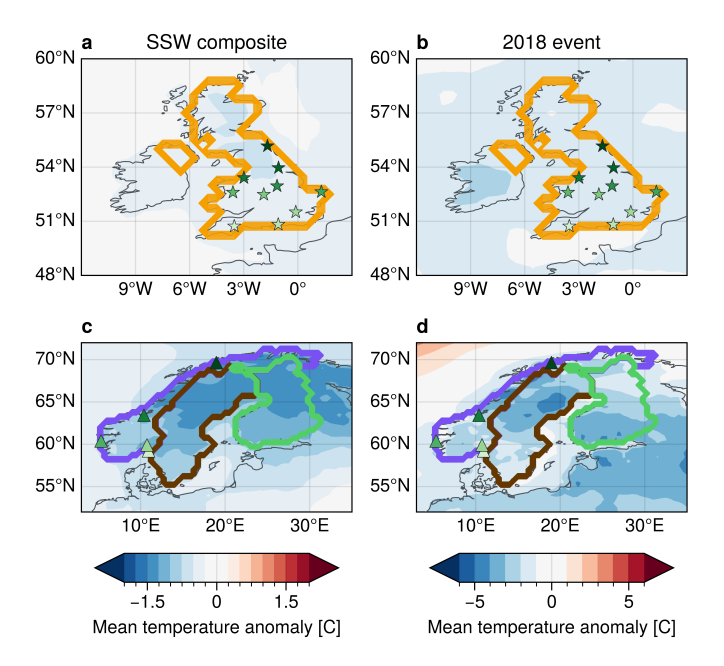


**Figure 1.** Climatological anomaly of 2-metre temperature for (a,b) the United Kingdom and (c,d) Northern Europe in re-analysis data. Left panels (a,c) show a composite mean averaged over 30 days following 41 SSW events between 1960 and 2023, right panels (b,d) show the average over 30 days following the 2018 SSW (note different colour scales). Markers show the locations used as representative for different regions in the UK and Norway (see Table 1). Coloured contour lines show the outlines of the countries of interest (United Kingdom, Norway, Sweden and Finland).

2013; Wang et al., 2016; Mistry et al., 2022). A widely used methodology to compute such exposure-response curves utilises Distributed Lag Non-linear Models (DLNMs) due to their capability to capture both nonlinear and delayed temperature effects (Gasparrini et al., 2011; Gasparrini and Armstrong, 2013). However, to accurately account for lag-relationships to short-term variations, DLNMs require high-temporal-resolution data (often daily), which may not be consistently available across different regions or periods. Such DLNM approaches further require various parameters to be optimised, which complicates the analysis practically. In this study, we further explore a different methodology in terms of a simple binning approach and demonstrate its potential to yield robust results even for monthly mean data.

To systematically quantify the mortality impacts of the 2018 SSW, we leverage ensemble simulation experiments from the Stratospheric Nudging and Predictable Surface Impacts (SNAPSI) project (Hitchcock et al., 2022). SNAPSI provides coordinated model experiments where the zonal-mean strength of the polar vortex is nudged either towards observed conditions (thus ensuring the presence of an SSW) or towards climatology (effectively removing the SSW signal). Comparing these two scenarios enables robust attribution of observed surface impacts and associated mortality to the SSW event. The use of such ensemble simulations over simple re-analysis composite further supports the feasibility of attribution studies and impact analyses when only coarse temporal impact datasets are available (e.g. monthly scale).





The structure of this paper is as follows: Section 2 gives a detailed overview of the utilised datasets and numerical models. In Section 3 we then introduce the general framework to assess attributable impacts of SSW events on mortality via exposure-response curves and nudged ensemble simulations. We further test the sensitivity of this framework with regard to different exposure-response model approaches and temporal resolution of the input mortality data. Afterwards, Section 4 applies the framework to assess the mortality impacts of the 2018 SSW for the UK and Nordics, with particular focus on the regional differences and relative risks compared to the spatially non-uniform temperature signal (see Figure 1). Finally, Section 5 briefly summarises and discusses the main conclusions of this study.

## 2 Data and numerical models

The attribution analysis presented in this study requires three types of datasets. First, we need observational temperature data covering a sufficiently long historical period to robustly construct exposure-response relationships between temperature anomalies and mortality risk. Second, corresponding mortality data for the same historical period is required. Finally, ensemble model forecasts of the 2018 SSW event is essential for quantifying the mortality impacts directly attributable to this stratospheric event. The following subsections detail each of these datasets, including their sources, spatial and temporal resolutions, and covered periods.

#### 2.1 Re-analysis data

100

The ERA5 re-analysis dataset (Hersbach et al., 2020) of the European Centre for Medium range Weather Forecasts (ECMWF) is used as the representation of atmospheric state. In particular, we use 2-metre temperature (t2m) provided on a  $0.5^{\circ} \times 0.5^{\circ}$  regular grid. All analyses are based on daily means, computed from 6-hourly data. Throughout the manuscript we use the period 1.1.1960 to 31.12.2018 as a reference to compute daily climatological means (smoothed with a 31-day running mean, to reduce high frequency sampling variability) and corresponding anomalies. For analyses where mortality is only given in a shorter period, we accordingly use fields and anomalies within the overlapping period. Sudden stratospheric warming event onset dates are based on the SSW compendium described in Butler et al. (2017).

Note that the temperature (and mortality) datasets used in this study potentially include long-term trends, e.g., due to climate change. We do not explicitly remove these trends before processing the data (cf. Figure 3). However, some of the methods we use (specifically the DLNM, see Section 3.1) uses a spline-interpolation to remove seasonal variations in the data. This will likely also remove part of any long-term trend included. Other methods (like the binning approach, see Section 3.2) do not remove any trends or seasonal variability. As we will show later, the good agreement between these two methods suggests that long-term trends do not affect our conclusions.

To define temperature time series for various regions of interest we use two approaches. For country-level analyses, we use the average temperature of all grid points within the corresponding borders. On the city and region level, we use a single representative point for the respective region. This point is chosen to be rather central within a county, and ideally close to a larger city, to obtain the strongest connection to potential mortality impacts. Using representative single points for regional





signals can be justified due to the generally large scale surface temperature structures within the ERA5 and model datasets (see Figures 1 and 2). Table 1 shows the choice of representative points for the different regions studied within Norway and the United Kingdom.

**Table 1.** Climatological and post-SSW characteristics for different regions in the UK and Norway. Shown are the latitude/longitude points used to extract time series for the individual regions, the climatological DJF-mean temperature and the composite mean temperature following 41 SSW events (1960-2023).

Region	Latitude [°N]	Longitude [°E]	DJF mean temperature [°C]	Post-SSW temperature anomaly [°C]
England+Wales				
North East England	55.2	-1.7	4.8	-0.5
Yorkshire and Humber	54.0	-1.1	4.0	-0.5
North West England	53.4	-3.0	5.6	-0.4
East Midlands	53.0	-1.2	4.4	-0.5
Wales	52.6	-3.6	3.4	-0.5
East of England	52.6	1.3	5.1	-0.4
West Midlands	52.5	-1.9	4.5	-0.4
London	51.5	-0.1	4.8	-0.4
South East England	50.8	-1.1	5.1	-0.4
South West England	50.7	-3.5	6.7	-0.3
Norway				
Tromsø	69.6	19.0	-8.9	-1.4
Trondheim	63.4	10.4	-3.3	-1.2
Bergen	60.4	5.3	-1.0	-0.8
Oslo	59.9	10.8	-4.4	-1.1
Fredrikstad	59.2	10.9	0.1	-0.9

# 2.2 Mortality data sources

Health impacts in this study are quantified in terms of excess mortality. Here, we use all-cause mortality in absolute numbers, typically collected from local health authorities and health institutions. The mortality data used in the present study was obtained from various sources, with different temporal and spatial resolutions and covered periods; see Table 2.

# 2.3 Model experiments

We use a set of ensemble re-forecasts conducted as part of the Stratospheric Nudging And Predictable Surface Impacts (SNAPSI) project. In particular, we use runs performed with 5 different modelling systems, all initialised on 25 January 2018



120



Table 2. Mortality datasets used in this study for the countries United Kingdom (UK), Norway (NO), Finland (FI) and Sweden (SE).

Country	Data source	Spatial level	Temporal resolution	Coverage	
UK,SE,NO,FI	EuroStat	Entire country	Monthly	1960-2018	https://ec.europa.eu/eurostat
UK	UK Office for Nat. Statistics	Wales + 9 English regions	Daily	1981-2018	https://www.ons.gov.uk/
NO	Norwegian Death Registry	6 cities + entire country	Daily	1996-2018	https://www.fhi.no/
FI	Statistics Finland	Entire country	Weekly	1990-2018	https://stat.fi
SE	EUROMOMO	Entire country	Weekly	2017+2018	https://www.euromomo.eu/

(with observed SSW onset on February 12). The SNAPSI simulations include a nudging of the stratospheric zonal mean zonal wind and temperature (above 90hPa) to either the observed evolution during that time period ('nudged' experiment) or a climatological evolution ('control' experiment). Each experiment is run with 50 ensemble members. Correspondingly, in these model simulations all members either exhibit an SSW (in the nudged runs) or none of the members exhibit an SSW (in the control runs). Computing the difference between nudged and control experiments will therefore allow us to determine a statistically robust estimate of the influence of the SSW on the troposphere, independently of the intrinsic tropospheric variability.

Note that the SNAPSI project further provides simulations initialised on February 8, which we will not analyse in this study. While we do expect our results to be qualitatively similar for both initialisation dates, we focus on the earlier initialisation to ensure that the developing SSW does not affect the ensemble evolution and both nudged and control runs can be seen as 'plausible futures'. For more information about the model setups, see Table 3 and Hitchcock et al. (2022).

**Table 3.** Details of model setups within the SNAPSI project.

Forecast system	Spatial resolution	Model top	Reference
CNRM-CM61	TL359	0.01 hPa	Voldoire et al. (2019)
IFS	TCo319	0.01 hPa	IFS doc. (ECMWF)
CESM2-CAM6	$1.25^{\circ}$ x $0.9^{\circ}$	2 hPa	Richter et al. (2022)
GloSea6	N216	85 km	Williams et al. (2018)
CanESM5	T63	1 hPa	Swart et al. (2019)

The SNAPSI model experiments show a reasonable signature of SSW downward impact in terms of surface temperature field. Figure 2 compares the model surface temperature anomaly (as nudged-minus-control) to the climatological anomaly in re-analysis. All model runs show a pronounced cold anomaly over northern Europe, clearly covering Norway, Sweden and Finland. In some models this cold anomaly extends westward up to the UK, although other models show no or very weak anomalies here (consistent with observational variability). The model run with CESM2-CAM6 shows particularly strong temperature anomalies that extend very far west. However, note that this setup uses a rather low model top (2 hPa), which could explain the overestimation of the downward response due to misrepresentations of stratospheric processes.





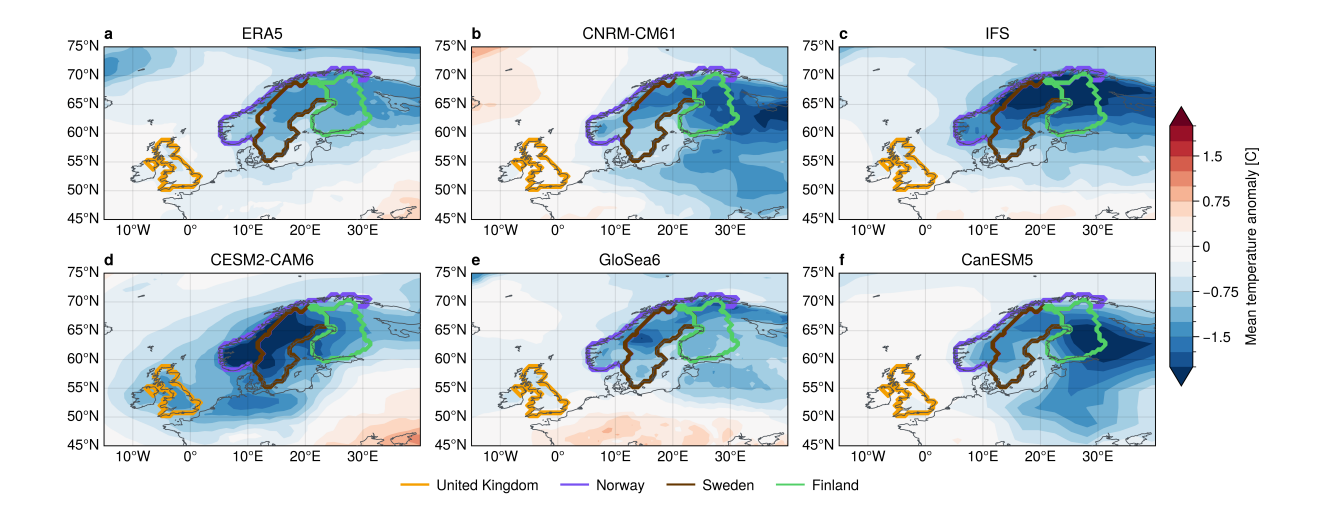


**Figure 2.** Composite mean anomaly of 2-metre temperature for part of Europe in (a) re-analysis data and (b-f) model simulations. Anomaly in re-analysis are computed w.r.t. climatology, anomalies for models are computed as difference between nudged and control experiments. All panels show the average over 30 days following the 2018 SSW onset. Coloured contour lines show the outlines of the countries of interest.

The good overall agreement between model signals and re-analysis gives confidence that this setup is suitable to study the potential mortality impact of the 2018 SSW in these regions.

#### 3 Methodology

## 3.1 Exposure-response curves from DLNMs

We quantify mortality attributed to SSW-related cold anomalies using a distributed lag non-linear model (DLNM), based on the R package discussed in Gasparrini et al. (2011). Various authors have previously used DLNM approaches to link temperature extremes to mortality impacts Guo et al. (2016); Vicedo-Cabrera et al. (2018); Lo et al. (2022). The DLNM is essentially a regression approach that characterises the temperature-mortality relationship, controlling for potential external effects like seasonal cycles and day-of-week. Temperature exposure is modeled with a 21-day lag period and five knots placed at the 10th, 25th, 50th, 75th, and 90th percentiles of the input data. These knots are points in the predictor distribution where the DLNM fit can change the properties of the underlying basis function and is hence used to determine the degrees of freedom and of the resulting function. Although we did not find a knot range between 3 and 7 to give substantially different results, the knot placement and density can in principle lead to over- or underfitting in different regions of the exposure-response curve.

Output of the DLNM is a relative risk (RR) curve, estimated with respect to the minimum mortality temperature (MMT).

The MMT is identified as the temperature associated with the lowest mortality risk for a given location. Absolute death counts attributable to temperature are then computed by multiplying the estimated RR with a baseline mortality, calculated as the



155

160



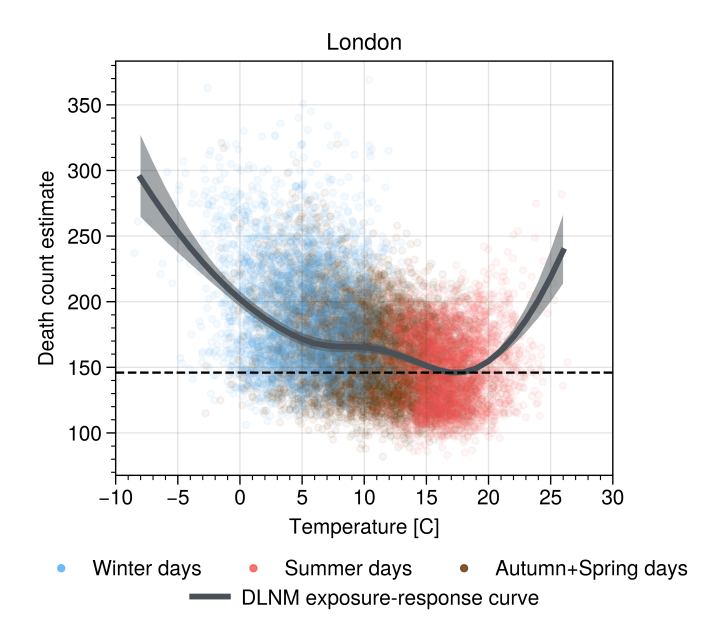


**Figure 3.** Mortality versus temperature for London. The gray line shows the exposure-response curve computed using a distributed-lag non-linear model (DLNM). Shading indicates the 95% confidence interval. Dots show daily death counts versus temperature on that day for the period 1981-2018, with colours representing the season. Horizontal dashed line indicates the baseline mortality corresponding to the MMT.

mean mortality within a  $\pm 1$  K bin around the MMT from the input mortality dataset. Bounds for the 95% confidence interval of mortality estimates are also derived from the model package.

Figure 3 illustrates the estimated temperature-mortality exposure-response curve compared to the direct temperature and mortality relationship on the same day (i.e. no lag), for winter, summer and shoulder-season days. It can be seen that much of the temperature-mortality relationship follows the general behaviour of the seasonal cycle, despite the DLNM controlling for seasonal variability. Note that the climatological spread in death counts (e.g. as standard deviation) for a fixed temperature bin also follows a similar qualitative shape (not shown), with minimum spread near the MMT and increasing spread for lower and higher temperatures.

Generally, the DLNM-derived exposure response curve captures an increased risk for cold and warm extremes. However, the spread of the underlying distribution is relatively large compared to the estimated confidence interval for the response curve. In particular for regional extreme temperatures (below -5° or above +25° for the case of London) the underlying exposure-response curve is mostly based on only a very few data points. The apparently high confidence of the model for these extreme values is, as can be argued, partly derived from inferring further information about the temperature-mortality relationship from more moderate temperature ranges, where ample data is available. However, the uncertainty remains large in these extreme ranges and it is not clear if the DLNM-derived curve is necessarily the best description of the underlying data.



170



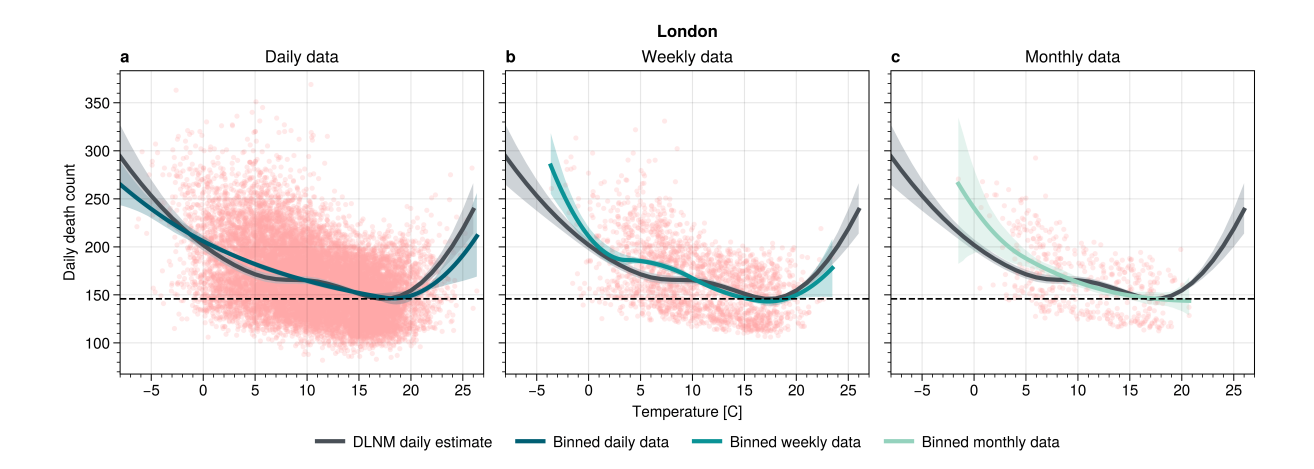


**Figure 4.** Exposure-response curves for London based on input data as (a) daily, (b) weekly and (c) monthly average. Red dots show death counts versus temperature distribution at the corresponding temporal resolution. Lines show the exposure-response curves using the DLNM or binned-data approach, with shading indicating the 95% confidence interval. The DLNM line is the same in every panel and is based on daily data only. Horizontal dashed lines indicate the baseline mortality corresponding to the MMT.

# 3.2 Robustness to model assumptions and data resolution

In section 3.1 we described how to obtain a exposure-response curve from using a DLNM. However, DLNMs are relatively complex and require a choice and optimisation of various model parameters (knots, control variables), as well as high-temporal-resolution data (often daily), to capture the lag-relationships. For some regions, we found that such daily mortality data is not available.

In this section we therefore investigate a simpler approach to obtain an exposure-repsonse curve, based on a binning method. Essentially, we define temperature bins with width of 2 K for the given range of values within a certain dataset (e.g. for London). We then average both mortality and temperature (extracted on the same day, i.e., with no lag) within each bin to obtain a single function of death count for a given temperature. To apply an additional smoothing, we fit a 3rd-over natural-spline to the resulting temperature-mortality curve, with knots at the 25th, 50th and 75th percentile of the binned data. Uncertainty bounds for the resulting exposure-response curve are computed via bootstrapping with 1000-draws from the original input data pool before applying the binning approach. (Note that we use the same bins, based on the original dataset, for each bootstrapping sample, for practical reasons).

Figure 4a illustrates that the exposure-response curves obtained from binning and DLNM approaches are generally in good agreement, with 95% confidence intervals overlapping for most sampled temperatures. Discrepancies are mostly present for extreme temperatures, where the underlying data uncertainty becomes large and it becomes difficult to argue that either of the models is a more accurate representation of the corresponding relationship.





185

190

195

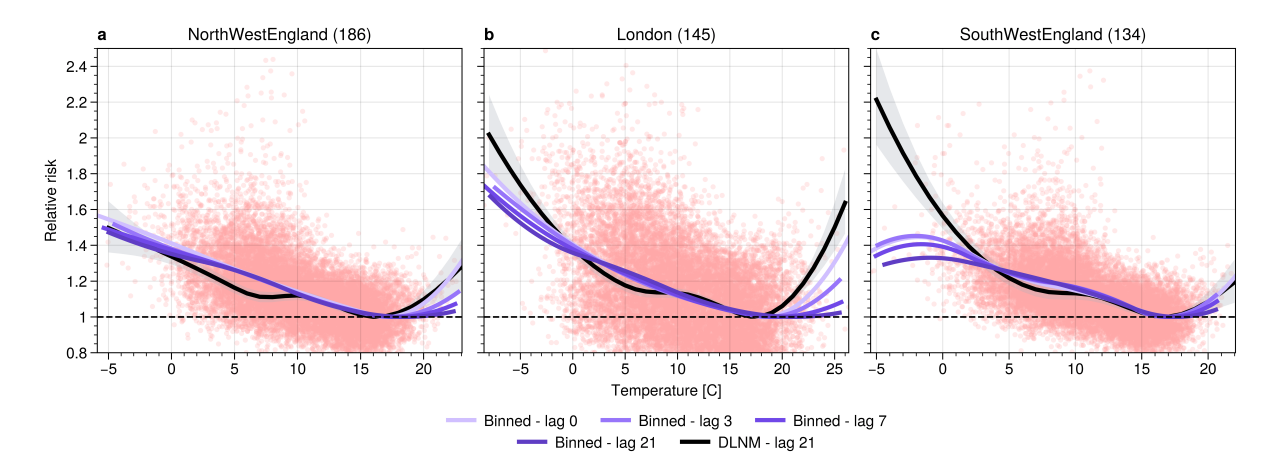


**Figure 5.** Exposure-response risk curves for three different regions in England based on daily data. Dots show the distribution of mortality risk versus temperature, with risk computed as death count normalised by the MMT base count (shown in brackets) and using no lag in all panels. Lines show the exposure-response curve based on the DLNM or the binning approach. The DLNM uses a lag of 21 days, for the binning approach is shown for varying lag between 0 and 21 days.

A main advantage of the binning approach is that it can be easily applied to almost any input dataset, including lower temporal resolution data. Figures 4b and 4c show the resulting exposure-response curves for London based on weekly and monthly input, respectively. Note that the displayed DLNM-derived curve is still computed from daily input data, as modifying the model for coarser-resolution data is non-trivial. While the overall temperature range narrows for aggregated data (since extreme temperatures become less frequent) the general shape of the response curve remains stable. Notably, the cold branch becomes steeper, which likely reflects a statistical compression effect: extreme daily values that drive mortality risk are smoothed out in aggregation, causing the same deaths to be concentrated into narrower temperature bins. However, we do find a general consistency between different model approaches (DLNM vs. binning) and temporal data resolutions (daily to monthly). This robustness across approaches and datasets does not only hold for London, but also other regions within the UK and the Nordics, like Oslo (Figure S1 in the supplement). The overall consistency and robustness of our analysis gives confidence in the methodology and supporting the framework's utility in data-limited settings.

As one of the main arguments for the use of DLNMs is often given the fact that it incorporates a lag-relationship, to capture delayed effects of short-term variations in the exposure variable. In principle, we can also include a lag-relationship in our binning approach. Figure 5 shows the sensitivity of the binning-derived exposure-response curves compared to the DLNM versions for three example regions in the UK. Here the lag is used to link the temperature on day t to the accumulated death count between days t and t+lag, similar to what is typically done within the DLNM (recall that we use a lag of 21 days within our DLNM). First, it can be seen that the cold branch of the exposure response curve stays robust, with no major dependency on the chosen lag for any of the three regions. For the examples of North West England and London (Figs. 5a and b), the binning-derived cold branches are in good agreement with the exposure-response curve obtained via the DLNM. For the



200

205

210

220

225

230



example of South West England (Fig. 5c) the binning-derived curves stay robust with respect to varying lags, but deviate from the DLNM-derived curve for extremely low temperatures (below about 0°C). However, the data coverage for these extremely low temperatures is very low and hence the exposure-response curve with strongly depend on the details of the underlying model like fitting parameters. Although one might argue that a decreasing mortality risk for extremely low temperatures seems unphysical, it is not *a priori* clear which of the models (DLNM or binning approach) gives a more appropriate simplified representation of the underlying data distribution. The deviation between the curves derived via different approaches can be considered as a 'model error', compared to the 'sampling error' that arises due to limited sampling (e.g. as indicated by shading in Fig. 4.

The warm branch of the binning-derived curves only show a steep increase with increasing temperatures for small or vanishing lags. In the case without lag the binning-derived curve closely follows the DLNM-derived curve while it stays rather flat and close to a relative risk of 1 when choosing larger lags. This behaviour could be explained as heat-related extremes are typically coupled to mortality on very short time scales Gasparrini and Armstrong (e.g. 2011). A heatstroke on a particularly hot day, for example, will lead to death on the same or the following days, but will hardly lead to a death 3 weeks after. Without controlling for long-term variability (as done in the DLNM), this could smooth-out the short-term effect of heatwaves when using long lags. Cold-related deaths, however, often occur from persistent cold temperatures, that sometimes do not necessarily require large magnitudes (Gasparrini et al., 2015; Wang et al., 2016; Keatinge et al., 2000, see, e.g.,). Hence, the cold branches of the curves stay less affected by temporal aggregation.

# 215 3.3 Demographic and regional variations in mortality risk for the UK

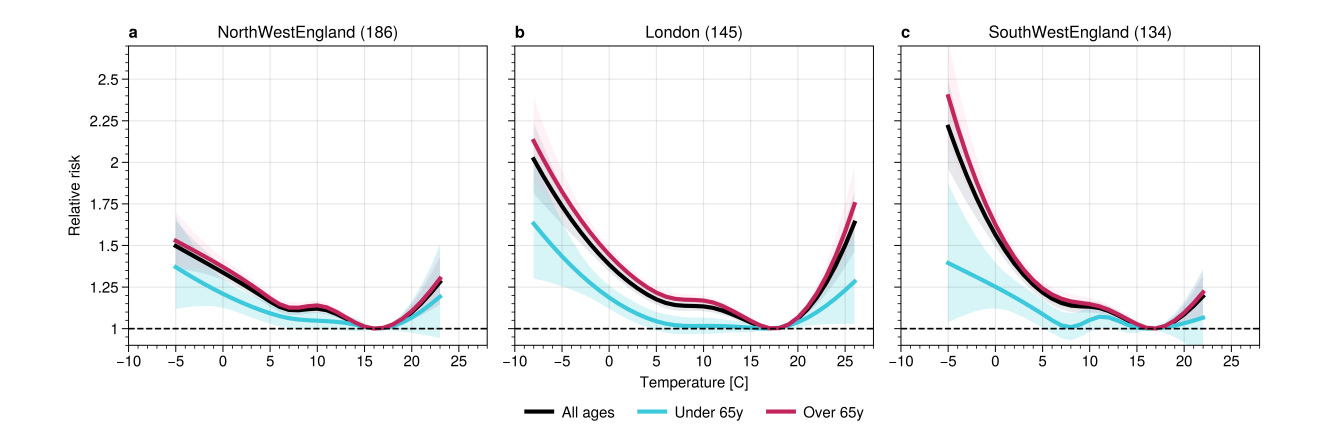
Mortality risk for cold anomalies is often a highly non-linear function of various parameters besides temperature itself. For example, demographic characteristics like age can strongly affect the impact of temperature anomalies on mortality. While younger people are usually very resilient to cold, older people can be highly vulnerable. However, the death risk for the younger population can still increase substantially for extreme cold values.

Figure 6 shows that, for example, the risk of death for people 65 years or younger increases by almost 50% in London, when temperatures reach -5° C (compared to the MMT value). For certain regions, like North West England, the difference in increased risk during cold periods is only marginally smaller for people below 65 years, compared to people above 65. This indicates that the impact of cold spells (e.g. following SSWs) is not restricted to the oldest parts of the population. In fact, depending on demographics and economic development, younger parts of the population can be even more vulnerable (Kysely et al., 2009).

In general, we find the cold branch of the mortality risk curve to be much steeper in some regions compared to others. In particular, there is a tendency for UK regions further south to be associated with much steeper curves than regions further north (see Fig. 7). This behaviour could be explained by the fact that northern regions are more used to experiencing cold conditions and their populations are therefore 'better adapted' to cold periods. Demographic differences between regions may also play a role. Although it might be surprising to see such a clear gradient on a regional scale, this finding is consistent with results







**Figure 6.** Exposure-response curves for mortality risk as function of temperature for three different regions in the UK. Curves show the mortality risk for all ages, and below/above 65 years. Shadings indicate the 95% confidence interval. Numbers in brackets give the baseline mortality count at MMT.

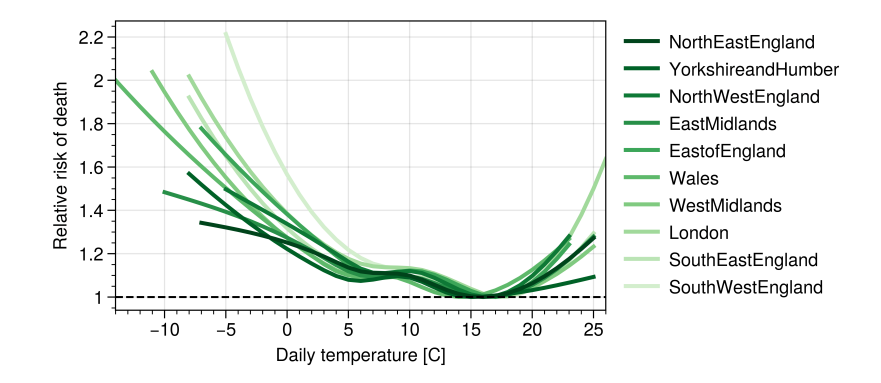


**Figure 7.** Exposure-response curves for mortality risk as function of temperature for different regions in the UK based on the DLNM approach. Regions are roughly sorted from North (dark colours) to South (light colours). The x-range of each curve is determined by the observed range of temperature values.

of other authors, who showed that European countries with higher climatological temperatures are usually more vulnerable to cold spells (Group, 1997).

#### 4 Results

## 4.1 Mortality impact of SSWs within the UK

To assess the impact of the February 2018 SSW on mortality in our numerical experiments (see Section 2.3) we use exposureresponse curves (as derived in Section 3.1). This way we can simply take the surface temperature output of the model to



245



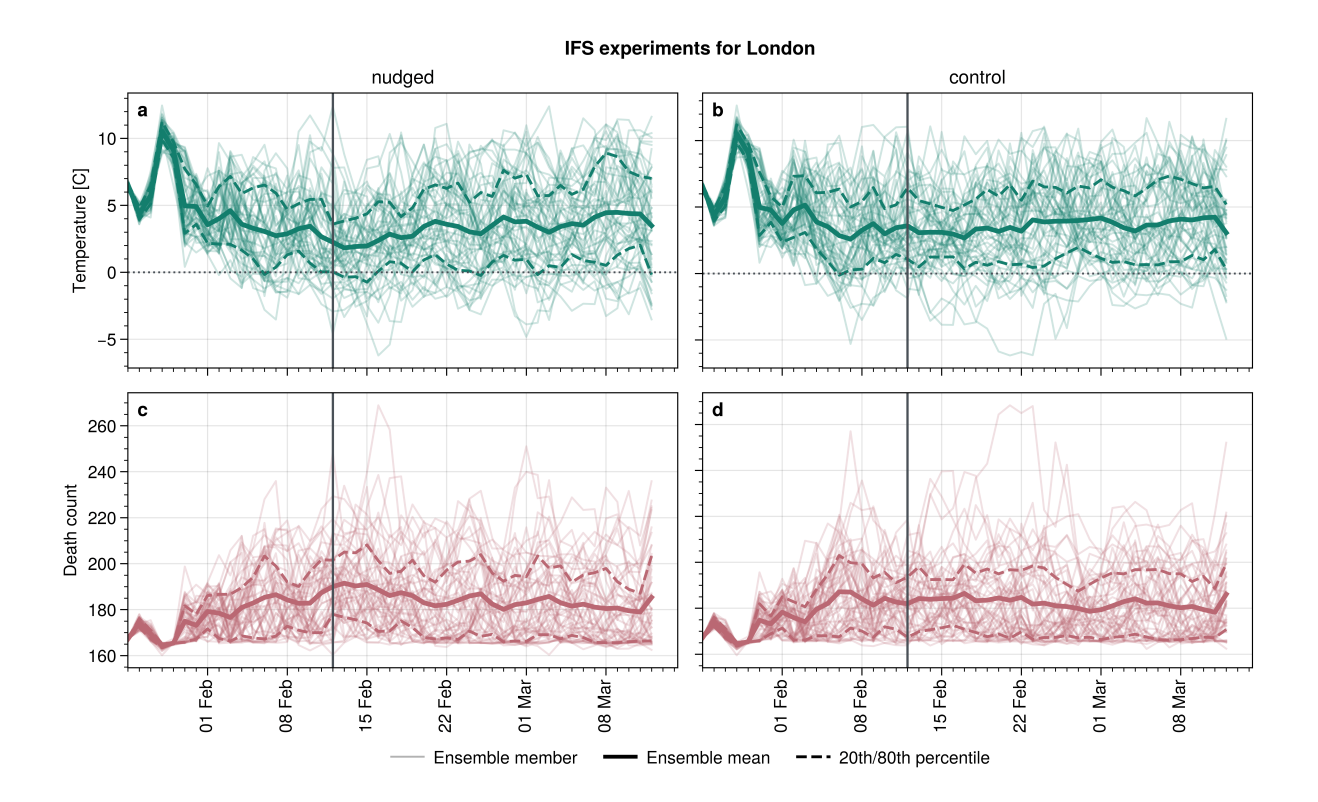


**Figure 8.** Example of an ensemble simulation for (a,b) temperature and (c,d) expected death count in London based on the IFS model. Shown are the nudged (a,c) and control (b,d) SNAPSI experiments. Death counts are computed from temperature using the DLNM exposure-response curve. Vertical solid lines indicate the SSW onset on February 12.

compute an expected death count within each simulation. Figure 8 illustrates an example of temperatures in London and the associated expected death counts for the nudged (with SSW) and control (without SSW) SNAPSI experiments obtained from the IFS model. Any differences between the nudged and control experiments in death counts can then be directly attributed to the occurrence of the SSW. However, note that we can only compare statistical properties of the ensemble distribution, and individual members cannot be compared.

Figure 9a shows a clear negative temperature anomaly in the MMM for London for essentially the entire covered period following the SSW (about 6 weeks). This anomaly reaches magnitudes of roughly 1K and can by construction be attributed to the SSW. Since the exposure-response curve for London steeply increases with decreasing temperatures (Fig. 3) this negative temperature anomaly is associated with a pronounced positive expected death rate anomaly which reaches about 4 deaths/day in early March. This increase in death rate leads to an estimated total number of excess deaths attributable to the SSW for London of 91, when averaged over the entire period after the SSW.

An analogous analysis as shown in Figure 9 can be performed for other UK regions and using the different approaches described above to derive the underlying exposure-response curves. Figure 10 compares the average increase in excess deaths







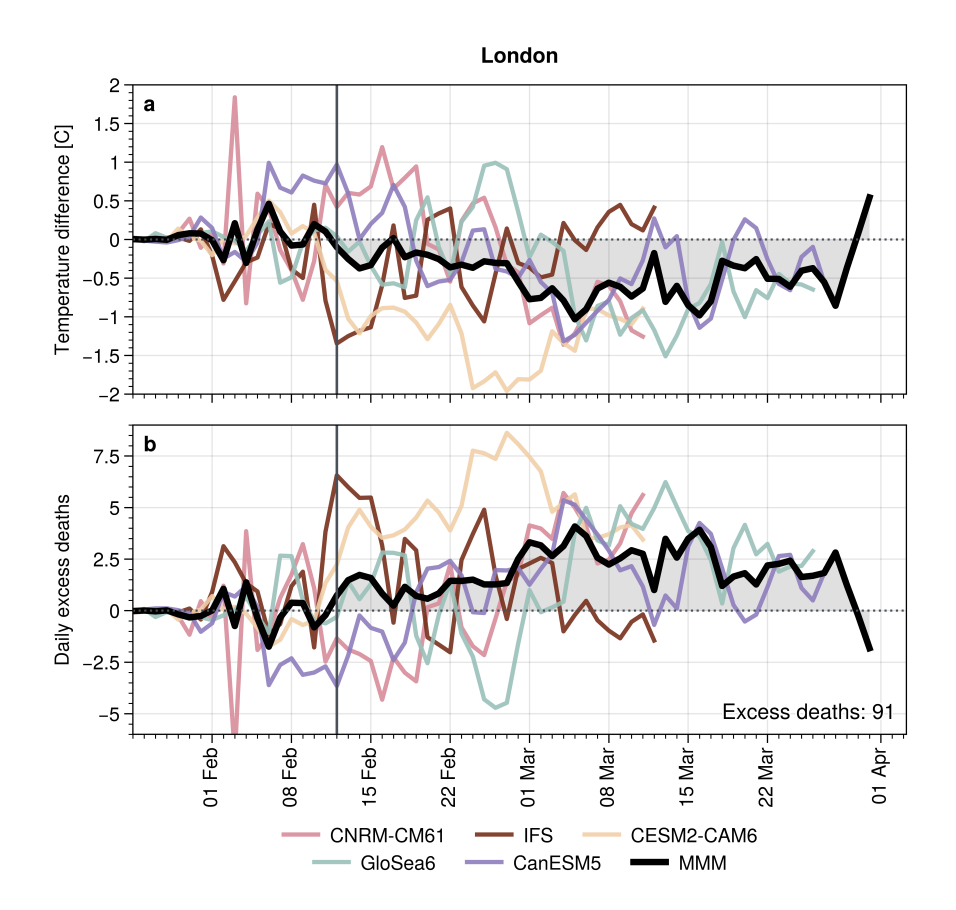


**Figure 9.** Difference in (a) temperature and (b) expected death count between nudged and control experiments for example of London and different models. Multi model mean is shown as thick black line with area between the curve and the x-axis being highlighted. Death counts are computed based on the DLNM exposure-response curve. Vertical solid lines indicate the SSW onset on February 12. Total excess deaths are computed as time average of the MMM from the SSW onset to March 31. Note that different models have different integration lengths and hence contribute differently to the MMM.

and relative risk attributable to the SSW for different UK regions, as well as temporal resolution of input data and exposure-response models (DLNM vs. binning approach). Note that we only consider the first 30 days following the SSW onset in Figure 10 to make different input temporal resolution easier to compare. The estimated death risk from the DLNM varies between about 0.7% in South East England and 1.6% in North West England. However, no clear north-south gradient is apparent.

Comparing the DLNM and binning approaches for daily input data shows a high degree of agreement, consistent with our findings from Figure 4a and giving further confidence in the validity of both methods. The results for estimated death count and risk anomalies also stay robust when weekly data is used. For some regions even monthly input data leads to very good estimates in high agreement with the higher-temporal-resolution inputs (e.g. South West England or East Midlands). However, using monthly inputs seems to overestimate the attributable impact by up to a factor of about 2 (in Yorkshire and Humber).





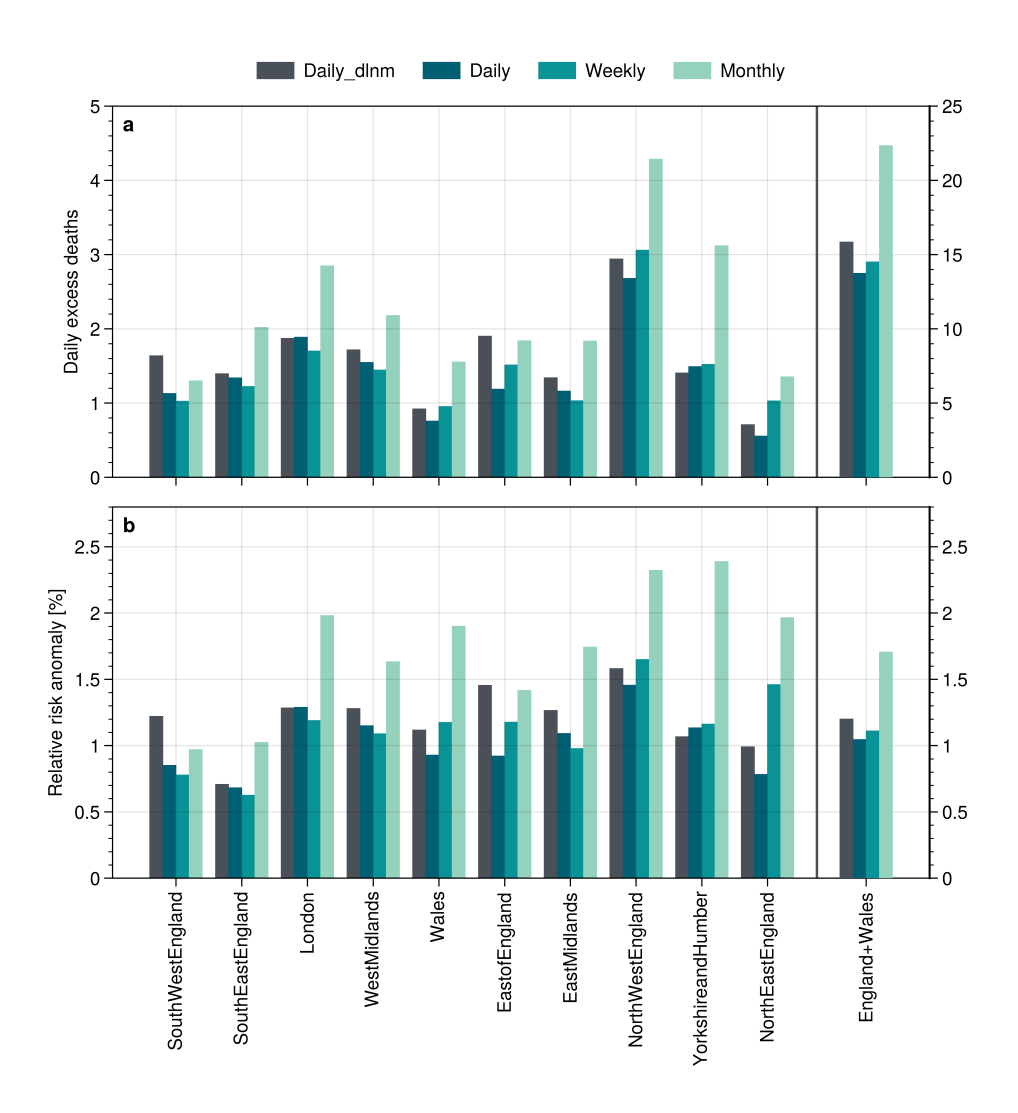


**Figure 10.** Attributable SSW impacts on mortality for different UK regions. Shown are (a) the daily excess deaths and (b) the relative risk anomaly, both estimated as MMM difference between nudged and control experiments and averaged over the 30 days following the SSW onset. Different bars are based on different exposure-response models, with the DLNM using daily input data and binning approach using daily, weekly, or monthly data. Total death rates for England+Wales are the sum of all regions, while the total risk anomaly is given as average over all regions.



260

280

285

290



Nevertheless, if no other data is available, monthly inputs still seem to give reasonable results of the same order of magnitude in this case.

On average, our analysis estimates the excess deaths attributable to the February 2018 SSW to be around 15 deaths per day throughout England and Wales for a period of 30 days, which is an increase of about 1% compared to the average winter-time death count.

### 4.2 Different impacts of SSWs between UK and the Nordics

To contrast the mortality analysis for the UK, this section applies our framework to the Nordic countries of Norway, Finland and Sweden. Figures 2 and 1 show that the post-SSW temperature anomaly is typically much stronger in these Nordic countries, compared to the UK. However, the magnitude of any mortality impacts is *a priori* not clear due to the strong degree of non-linearity in some of the exposure-response curves. In fact, the Nordic countries tend to be associated with rather flat exposure-response curves (Figure 11). The modelled daily mortality risk increases by about 20% in Norway and Finland and about 40% in Sweden for the most extreme cold anomalies recorded in our dataset relative to the risk at the MMT. These numbers compare to risk increases ranging from 40% to 120% for individual regions in the UK (Figure 7) based on daily data. Note that the exposure-response curves for UK are also steeper than the ones for the Nordics for purely monthly data (Figure S2 in the supplement). Another significant difference between the UK and Nordic mortality curves is the MMT itself, with MMT in the UK being about 5 to 10 K warmer compared to the Nordic countries. However, this shift in MMT alone does not seem to explain the resulting differences in attributable mortality without an additional change in steepness.

The differences in shape of the exposure-response curves then translate into non-trivial differences between estimated excess deaths for the different countries. Figure 12 compares the decrease in temperature and the associated increase in mortality risk following the SSW in the UK and different Nordic countries based on different mortality models and input temporal resolutions (note that certain UK datasets only assess the risk for England and Wales). Overall, the UK shows robustly weak mean temperature anomalies of about -0.5 K compared to anomalies exceeding -1 K throughout the Nordics and reaching up to -1.5 K. However, the mortality risk increase in the UK is estimated to be at least as strong (if not stronger) than in the Nordics. While the UK shows an increased risk of 1% or more, most estimates for the Nordic countries stay below 1%. Although estimates vary for different model types and input datasets, the overall results are robust. All regions show positive risk anomalies due to the negative temperature signals associated with the SSW.

The effect of the SSW on absolute death counts are quantified in Table 4, showing best-estimates based on the highest available temporal resolution data and the DLNM approach where daily data was available. The estimates are based on the full period following the SSW with avavailable model data, i.e., Feb. 12 to Mar. 31 (in contrast to some earlier results based on 30 days post-SSW). we find that about 750 deaths in England and Wales were attributable to the impact of the February 2018 SSW. In contrast, a combined count of about 250 deaths in the Nordic countries Finland, Sweden and Norway could be attributed to the SSW.





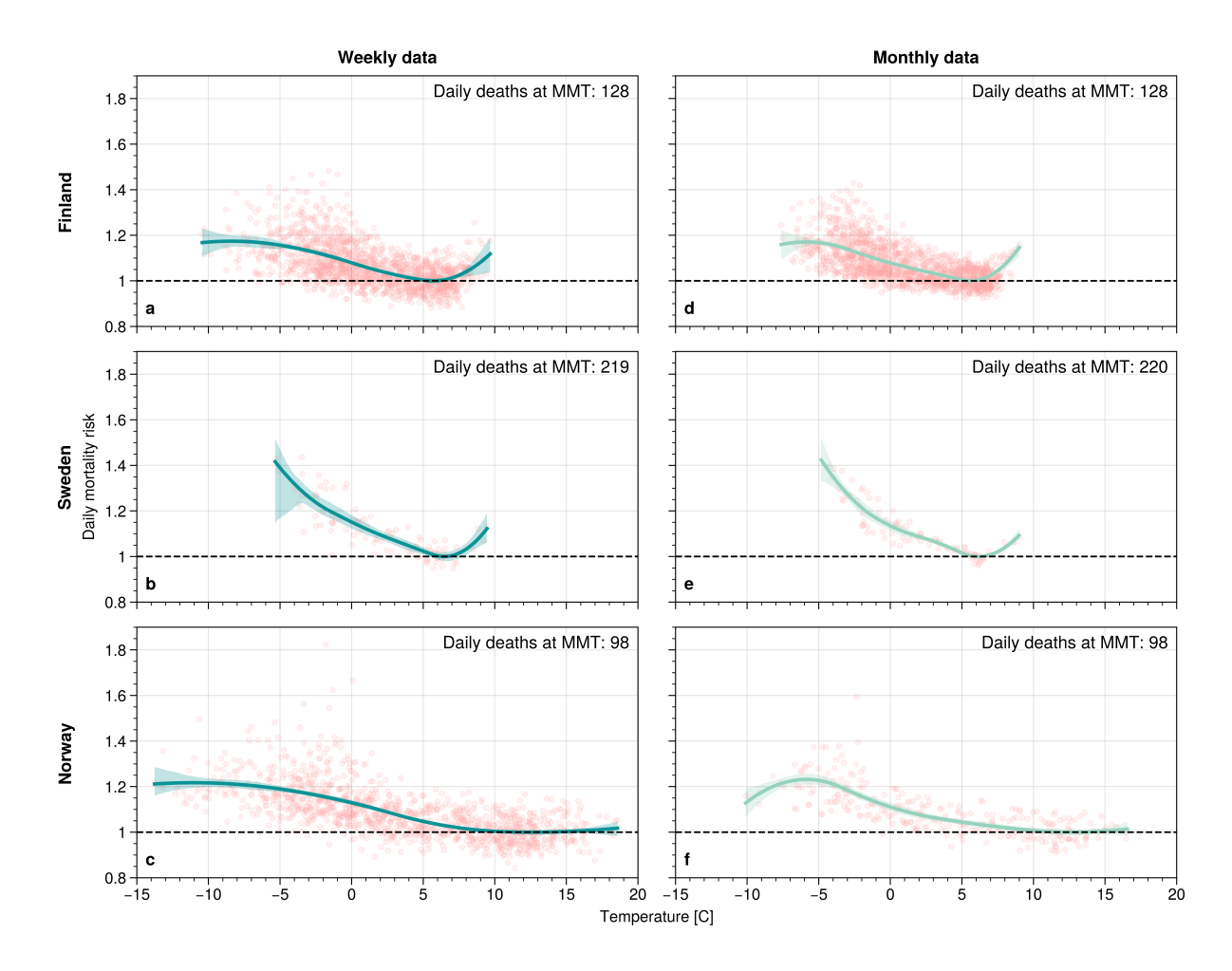


**Figure 11.** Exposure-response curves derived from the binning approach for (a,d) Finland (b,e) Sweden and (c,f) Norway based on input data with (a,b,c) weekly or (d,e,f) monthly mean temporal resolution. Red dots show death counts versus temperature distribution at the corresponding temporal resolution and location. Shading indicated the 95% confidence interval around the curve. Note that for daily data is available for Norway but not shown. Monthly means for Sweden and Finland are computed from weekly data as 4-week running mean. Weekly and monthly data for Norway is computed as direct average over fixed week-of-year or month-of-year bins.





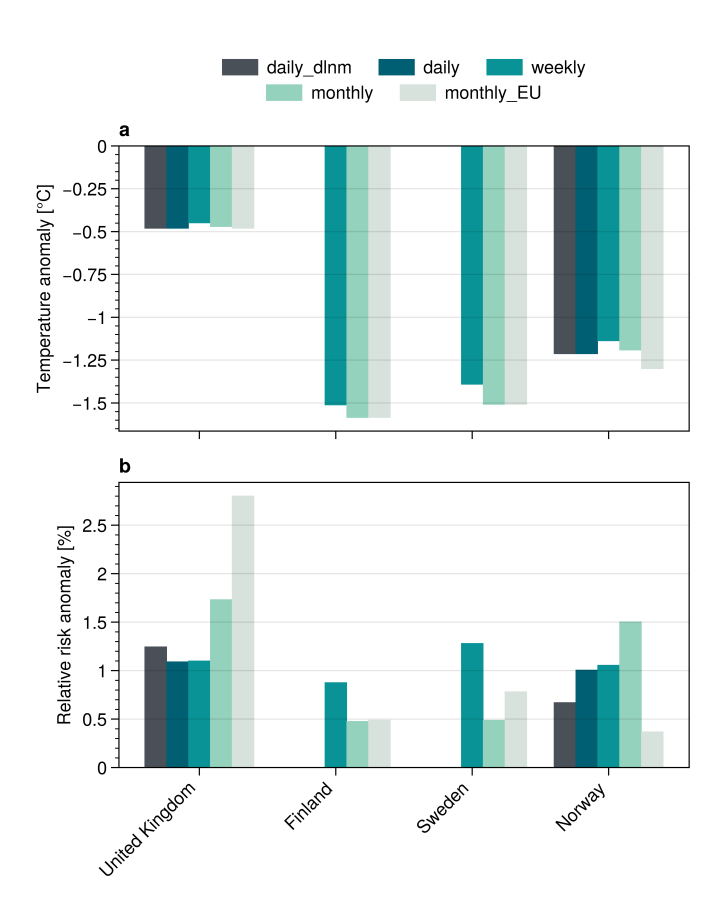


Figure 12. Meteorological and socio-economic impacts in the 30 days following the SSW. a) Temperature anomaly and b) mortality risk anomaly for different countries. All data is given as difference of nudged and control experiments with mortality computed via exposure-response curves based input data with different temporal resolutions and different model approaches (DLNM or binning). Anomalies are computed from daily, weekly or monthly data, based on availability. Note that the EUROSTATS dataset includes data for the entire United Kingdom, while all other UK datasets only contain England+Wales. Further recall that the different datasets cover different time period.

**Table 4.** Estimated deaths and changes in mortality risk attributable to the 2018 SSW in different regions for specific model and dataset combinations.

Region	Temporal resolution/model	Attributable excess deaths	Attributable risk increase [%]
England+Wales	daily/dlnm	758	1.2
Finland	weekly/binning	56	0.9
Sweden	weekly/binning	160	1.3
Norway	daily/dlnm	31	0.7



295

300

305

310

315

320



#### 5 Discussion and conclusions

This study presents a framework to attribute health impacts to meteorological phenomena, applying it specifically to the February 2018 SSW event and its associated cold surface anomalies. By combining exposure-response curves with stratospherically nudged ensemble forecasts, we demonstrate a robust method to quantify the mortality impacts attributable to stratospheric variability. Our findings suggest that at least 750 deaths in England and Wales and approximately 250 deaths in the Nordic countries can be linked to the post-SSW temperature anomalies of 2018 (Table 4). Here, our estimate might pose a lower bound on the actual number of attributable deaths, as we are restricted by the finite length of the numerical ensemble simulations. Figure 9 suggests that temperature and mortality signals could still be present after March 31st. The actual number of deaths attributable to the strong SSW event in early 2018 might be even higher. However, note that our attributed mortality impact for the UK is generally consistent with the mean SSW mortality impact of 620 deaths found by Charlton-Perez et al. (2021).

Our analysis underlines that the relationship between temperature anomalies and mortality risk is non-trivial and often highly non-linear (e.g., Gasparrini et al., 2015), and further shows that these characteristics also apply to cold anomalies associated with stratospheric variability. Although the Nordic countries experienced the strongest post-SSW temperature drops, the attributable increase in mortality risk in the UK was overall higher (Fig. 12). This can be understood through the highly non-linear shape of the exposure-response relationship, with extremely steep cold branches in regions less adapted to cold conditions. For instance, we find a clear north-south gradient within the UK, where southern regions such as London and South West England show a sharper increase in mortality risk at lower temperatures than their northern counterparts (Fig. 7). A similar pattern is observed at the city level in Norway, with Bergen exhibiting an unusually steep cold-branch response compared to the other cities studied (Fig. S3 in the supplement), potentially due to its typically mild, ocean-moderated winter climate. Nevertheless, we do not find such a clear overall north-south gradient in Norway.

Interestingly, while the exposure-response curves for southern UK regions tend to be steeper, the resulting risk anomalies are not systematically larger than those in the north (Fig. 10). One reason might be that the increased steepness of the exposure-response cold branch towards the south compensates for the generally smaller post-SSW temperature anomalies observed in these regions (Fig. 2). This balance further highlights the need to consider both hazard magnitude and population vulnerability when assessing health impacts. Beyond climatological adaptation, demographic or socioeconomic factors may also play a role in shaping regional differences. Such factors could comprise of baseline health conditions, urban heat retention, or heating practices, although the precise role of additional influences remains beyond the scope of the current dataset and merits further targeted investigation.

Methodologically, we show that the presented framework is flexible and yields consistent results across different modeling approaches and data resolutions (e.g. Fig. 10). While DLNMs offer a theoretically grounded estimate of the lagged mortality response, our simpler binning-based method also proves effective, even when applied to coarser temporal inputs such as weekly or monthly mortality data. This robustness is encouraging, especially in light of the often-limited availability or quality of health data in many regions. Moreover, the fact that even monthly data can yield meaningful estimates implies that this method could be applied in data-sparse contexts or retrospectively using long-term archives.



330

335

345

350



We note, however, that uncertainties in the construction of exposure-response curves remain large. These include sensitivity to choice of statistical model, temporal aggregation and lag assumptions, particularly for extreme temperatures where sample sizes are small. This is especially relevant in smaller regions such as individual Norwegian cities (Fig. S4 in the supplement), where daily death counts often remain in the single digits and introduce considerable statistical noise.

Our attribution analysis specifically studies the February 2018 event, chosen due to its pronounced temperature anomalies and clear societal impacts. However, attributing impacts across the broader distribution of SSW events requires careful consideration. While composite mean temperature anomalies averaged over multiple SSWs (cf. Fig. 2) can provide a general indication of expected impacts, they might underestimate the actual societal consequences. Mortality and other health impacts tend to be disproportionately influenced by extreme temperature anomalies rather than mean conditions. Particularly severe SSW events (like in early 2018) likely dominate the statistics on cumulative mortality impacts. Robust attribution of these disproportionate impacts require ensemble approaches similar to the one employed here (i.e. SNAPSI experiments), as such methods effectively isolate and quantify the contribution of individual, high-impact SSW events.

While this study focuses primarily on mortality impacts, SSW-triggered cold spells also carry substantial consequences for broader societal sectors, including transportation, energy demand, agriculture, and economic productivity (e.g., Büeler et al., 2020). Extending the presented analytical approaches to these sectors could enhance preparedness and adaptation strategies, especially where risk relationships are similarly non-linear. In particular, our findings on regional variation in exposure-response steepness may offer valuable insights for climate adaptation planning.

Future research could also apply the framework more broadly across Europe to assess SSW-related mortality in additional regions (analogous to, e.g., Analitis et al., 2008). The ability to obtain robust estimates even from monthly mortality data facilitates such large-scale studies, even in data-limited settings. Furthermore, complementing all-cause mortality with metrics such as years of life lost (YLL) or cause-specific impacts (e.g. respiratory illness) may help better capture the socio-demographic variation in vulnerability (e.g., Arbuthnott et al., 2020). In addition, methodologies such as the fractional attributable risk (FAR) approach could allow to extract attribution signals from re-forecast datasets without the need for nudging or other manipulation of the numerical model. Spaeth and Birner (2021), for example, used the FAR approach to statistically attribute Arctic Oscillation extremes to stratospheric events. Combining different approaches (like nudged experiments and FAR) could further enhance the scalability and applicability of our attribution framework.

Two important considerations apply to our use of stratospherically nudged ensemble forecasts. First, while this approach effectively isolates the downward influence of SSWs, the stratosphere-troposphere coupling is inherently bidirectional. Nudging the zonal-mean wind suppresses some of the upward feedback from the troposphere, which may lead to slightly unphysical evolutions near the SSW onset (Hitchcock et al., 2022). Second, the results are likely sensitive to the forecast initialisation date. Runs initialised too close to the SSW may not allow sufficient time for stratospheric signals to influence the troposphere. Our choice of January 25 offers a compromise, ensuring that both the nudged and control scenarios represent plausible futures in which downward propagation of the stratospheric signal could occur.

Overall, we think that our analysis framework represents a promising tool for the attribution of weather-related societal impacts. While applied here to cold spells triggered by a specific SSW event, the approach is generalizable to other meteorological

https://doi.org/10.5194/egusphere-2025-4587 Preprint. Discussion started: 11 November 2025

© Author(s) 2025. CC BY 4.0 License.



EGUsphere Preprint repository

drivers such as heatwaves, precipitation extremes, or air pollution events. The methodological approach offers a flexible basis for analysing impacts across diverse spatial and temporal contexts, helping to bridge atmospheric variability with real-world

societal risks in a policy-relevant way.

Code and data availability. Detailed information on the utilised datasets is given in Section 2 and our methodology is described in Section

3. While the re-analysis dataset is puplically available for download (ECMWF, 2018) access to output from the the SNAPSI experiments may

be obtained via request to the project leads (see Hitchcock et al., 2022). Access to the different mortality datasets can be restricted and is

detailed in Section 2.2.

365

370

375

Acknowledgements. We are highly grateful to Dann Mitchell and Eunice Lo for supplying the mortality data for England and Wales and

useful discussions about methodologies, as well as to Ilias Galanisto for supplying mortality data for Sweden from the EUROMOMO

dataset. We further want to thank the leads of the SNAPSI project Peter Hitchcock, Amy Butler and Chaim Garfinkel for access to the

model experiments. This work used JASMIN, the UK's collaborative data analysis environment (https://www.jasmin.ac.uk). We thank the

EXHAUSTION project (https://www.exhaustion.eu/) for providing the Norwegian data used in this study.

Author contributions. PR developed the analysis framework, performed most of the analyses and interpretation of results, coordinated the

different data sources and wrote the manuscript. LVF provided and processed data, constructed the exposure-response curves for Norway,

and helped revise the manuscript. WJMS assisted in conceptualising the analysis framework and interpreting the results, incorporating the

SNAPSI model data, and revising the manuscript. TB advised on the statistical handling of the datasets and assisted with interpreting the

results, forming the storyline and revising the manuscript.

Competing interests. The authors declare that they have no conflict of interest.

21





#### References

- Analitis, A., Katsouyanni, K., Biggeri, A., Baccini, M., Forsberg, B., Bisanti, L., Kirchmayer, U., Ballester, F., Cadum, E., Goodman, P., et al.: Effects of cold weather on mortality: results from 15 European cities within the PHEWE project, American journal of epidemiology, 168, 1397–1408, 2008.
  - Arbuthnott, K., Hajat, S., Heaviside, C., and Vardoulakis, S.: Years of life lost and mortality due to heat and cold in the three largest English cities, Environment international, 144, 105 966, 2020.
  - Baldwin, M. P. and Dunkerton, T. J.: Stratospheric harbingers of anomalous weather regimes, Science, 294, 581-584, 2001.
- Baldwin, M. P., Stephenson, D. B., Thompson, D. W., Dunkerton, T. J., Charlton, A. J., and O'Neill, A.: Stratospheric memory and skill of extended-range weather forecasts, Science, 301, 636–640, 2003.
  - Baldwin, M. P., Ayarzagüena, B., Birner, T., Butchart, N., Butler, A. H., Charlton-Perez, A. J., Domeisen, D. I., Garfinkel, C. I., Garny, H., Gerber, E. P., et al.: Sudden stratospheric warmings, Reviews of Geophysics, 59, e2020RG000708, 2021.
- Büeler, D., Beerli, R., Wernli, H., and Grams, C. M.: Stratospheric influence on ECMWF sub-seasonal forecast skill for energy-industryrelevant surface weather in European countries, Quarterly Journal of the Royal Meteorological Society, 146, 3675–3694, 2020.
  - Büeler, D., Ferranti, L., Magnusson, L., Quinting, J. F., and Grams, C. M.: Year-round sub-seasonal forecast skill for Atlantic–European weather regimes, Quarterly Journal of the Royal Meteorological Society, 147, 4283–4309, 2021.
  - Butler, A. H., Sjoberg, J. P., Seidel, D. J., and Rosenlof, K. H.: A sudden stratospheric warming compendium, Earth System Science Data, 9, 63–76, 2017.
- 395 Charlton-Perez, A. J., Huang, W. T. K., and Lee, S. H.: Impact of sudden stratospheric warmings on United Kingdom mortality, Atmospheric Science Letters, 22, e1013, 2021.
  - Domeisen, D. I. V., Butler, A. H., Charlton-Perez, A. J., Ayarzagüena, B., Baldwin, M. P., Dunn-Sigouin, E., Furtado, J. C., Garfinkel, C. I., Hitchcock, P., Karpechko, A. Y., Kim, H., Knight, J., Lang, A. L., Lim, E.-P., Marshall, A., Roff, G., Schwartz, C., Simpson, I. R., Son, S.-W., and Taguchi, M.: The Role of the Stratosphere in Subseasonal to Seasonal Prediction: 2. Pre-
- dictability Arising From Stratosphere-Troposphere Coupling, Journal of Geophysical Research: Atmospheres, 125, e2019JD030923, https://doi.org/https://doi.org/10.1029/2019JD030923, e2019JD030923 10.1029/2019JD030923, 2020.
  - ECMWF: IFS documentation, https://www.ecmwf.int/en/publications/ifs-documentation, accessed: 2025-09-14.
  - ECMWF: ERA5 database, https://www.ecmwf.int/en/forecasts/dataset/ecmwf-reanalysis-v5, accessed: 2025-09-14, 2018.
  - Gasparrini, A. and Armstrong, B.: The impact of heat waves on mortality, Epidemiology, 22, 68-73, 2011.
- 405 Gasparrini, A. and Armstrong, B.: Reducing and meta-analysing estimates from distributed lag non-linear models, BMC medical research methodology, 13, 1–10, 2013.
  - Gasparrini, A., Armstrong, B., and Scheipl, F.: Distributed lag linear and non-linear models in R: the package dlnm, Journal of Statistical Software, 43, 1–20, https://doi.org/10.18637/jss.v043.i08, 2011.
- Gasparrini, A., Guo, Y., Hashizume, M., Lavigne, E., Zanobetti, A., Schwartz, J., Tobias, A., Tong, S., Rocklöv, J., Forsberg, B., et al.:

  Mortality risk attributable to high and low ambient temperature: a multicountry observational study, The lancet, 386, 369–375, 2015.
  - Greening, K. and Hodgson, A.: Atmospheric analysis of the cold late February and early March 2018 over the UK, Weather, 74, 79–85, 2019.
  - Group, T. E.: Cold exposure and winter mortality from ischaemic heart disease, cerebrovascular disease, respiratory disease, and all causes in warm and cold regions of Europe, The Lancet, 349, 1341–1346, 1997.





- Guo, Y., Gasparrini, A., Armstrong, B. G., Tawatsupa, B., Tobias, A., Lavigne, E., Coelho, M. d. S. Z. S., Pan, X., Kim, H., Hashizume, M., et al.: Temperature variability and mortality: a multi-country study, Environmental health perspectives, 124, 1554–1559, 2016.
  - Hajat, S., Vardoulakis, S., Heaviside, C., and Eggen, B.: Climate change effects on human health: projections of temperature-related mortality for the UK during the 2020s, 2050s and 2080s, J Epidemiol Community Health, 68, 641–648, 2014.
  - Hersbach, H., Bell, B., Berrisford, P., Hirahara, S., Horányi, A., Muñoz-Sabater, J., Nicolas, J., Peubey, C., Radu, R., Schepers, D., et al.: The ERA5 global reanalysis, Quarterly Journal of the Royal Meteorological Society, 146, 1999–2049, 2020.
- 420 Hitchcock, P., Butler, A., Charlton-Perez, A., Garfinkel, C. I., Stockdale, T., Anstey, J., Mitchell, D., Domeisen, D. I., Wu, T., Lu, Y., et al.: Stratospheric Nudging And Predictable Surface Impacts (SNAPSI): a protocol for investigating the role of stratospheric polar vortex disturbances in subseasonal to seasonal forecasts, Geoscientific Model Development, 15, 5073–5092, 2022.
  - Huang, C., Barnett, A. G., Wang, X., and Tong, S.: Effects of extreme temperatures on years of life lost for cardiovascular deaths: a time series study in Brisbane, Australia, Circulation: Cardiovascular Quality and Outcomes, 5, 609–614, 2012.
- Huang, J., Hitchcock, P., Maycock, A. C., McKenna, C. M., and Tian, W.: Northern hemisphere cold air outbreaks are more likely to be severe during weak polar vortex conditions, Communications Earth & Environment, 2, 147, 2021.
  - Kautz, L.-A., Polichtchouk, I., Birner, T., Garny, H., and Pinto, J. G.: Enhanced extended-range predictability of the 2018 late-winter Eurasian cold spell due to the stratosphere, Quarterly Journal of the Royal Meteorological Society, 146, 1040–1055, 2020.
- Keatinge, W. R., Donaldson, G. C., Cordioli, E., Martinelli, M., Kunst, A. E., Mackenbach, J. P., Nayha, S., and Vuori, I.: Heat related mortality in warm and cold regions of Europe: observational study, Bmj, 321, 670–673, 2000.
  - King, A. D., Butler, A. H., Jucker, M., Earl, N. O., and Rudeva, I.: Observed relationships between sudden stratospheric warmings and European climate extremes, Journal of Geophysical Research: Atmospheres, 124, 13 943–13 961, 2019.
  - Kolstad, E. W., Breiteig, T., and Scaife, A. A.: The association between stratospheric weak polar vortex events and cold air outbreaks in the Northern Hemisphere, Quarterly Journal of the Royal Meteorological Society, 136, 886–893, 2010.
- 435 Kretschmer, M., Coumou, D., Agel, L., Barlow, M., Tziperman, E., and Cohen, J.: More-persistent weak stratospheric polar vortex states linked to cold extremes, Bulletin of the American Meteorological Society, 99, 49–60, 2018.
  - Kysely, J., Pokorna, L., Kyncl, J., and Kriz, B.: Excess cardiovascular mortality associated with cold spells in the Czech Republic, BMC public health, 9, 1–11, 2009.
- Lo, Y. E., Mitchell, D. M., Thompson, R., O'Connell, E., and Gasparrini, A.: Estimating heat-related mortality in near real time for national heatwave plans, Environmental research letters, 17, 024 017, 2022.
  - Lowe, R., Ballester, J., Creswick, J., Robine, J.-M., Herrmann, F. R., and Rodó, X.: Evaluating the performance of a climate-driven mortality model during heat waves and cold spells in Europe, International journal of environmental research and public health, 12, 1279–1294, 2015.
- Mistry, M. N., Schneider, R., Masselot, P., Royé, D., Armstrong, B., Kyselỳ, J., Orru, H., Sera, F., Tong, S., Lavigne, É., et al.: Comparison of weather station and climate reanalysis data for modelling temperature-related mortality, Scientific reports, 12, 5178, 2022.
  - Overland, J., Hall, R., Hanna, E., Karpechko, A., Vihma, T., Wang, M., and Zhang, X.: The polar vortex and extreme weather: the Beast from the East in winter 2018, Atmosphere, 11, 664, 2020.
  - Pyrina, M., Vicedo-Cabrera, A. M., Büeler, D., Sivaraj, S., Spirig, C., and Domeisen, D. I.: Subseasonal prediction of heat-related mortality in Switzerland, GeoHealth, 9, e2024GH001 199, 2025.
- 450 Richter, J. H., Glanville, A. A., Edwards, J., Kauffman, B., Davis, N. A., Jaye, A., Kim, H., Pedatella, N. M., Sun, L., Berner, J., et al.: Subseasonal Earth system prediction with CESM2, Weather and Forecasting, 37, 797–815, 2022.





- Sarofim, M. C., Saha, S., Hawkins, M. D., Mills, D. M., Hess, J., Horton, R., Kinney, P., and Schwartz, J.: Ch. 2: Temperature-Related Death and Illness, Tech. rep., Washington, DC, https://doi.org/10.7930/J0MG7MDX, 2016.
- Spaeth, J. and Birner, T.: Stratospheric modulation of Arctic Oscillation extremes as represented by extended-range ensemble forecasts,
  Weather and Climate Dynamics Discussions, 2021, 1–25, 2021.
  - Spaeth, J., Rupp, P., Garny, H., and Birner, T.: Stratospheric impact on subseasonal forecast uncertainty in the Northern extratropics, Communications Earth & Environment, 5, 126, 2024.
  - Swart, N. C., Cole, J. N., Kharin, V. V., Lazare, M., Scinocca, J. F., Gillett, N. P., Anstey, J., Arora, V., Christian, J. R., Hanna, S., et al.: The Canadian earth system model version 5 (CanESM5. 0.3), Geoscientific Model Development, 12, 4823–4873, 2019.
- Vicedo-Cabrera, A. M., Guo, Y., Sera, F., Huber, V., Schleussner, C.-F., Mitchell, D., Tong, S., Coelho, M. d. S. Z. S., Saldiva, P. H. N., Lavigne, E., et al.: Temperature-related mortality impacts under and beyond Paris Agreement climate change scenarios, Climatic change, 150, 391–402, 2018.
  - Voldoire, A., Saint-Martin, D., Sénési, S., Decharme, B., Alias, A., Chevallier, M., Colin, J., Guérémy, J.-F., Michou, M., Moine, M.-P., et al.: Evaluation of CMIP6 deck experiments with CNRM-CM6-1, Journal of Advances in Modeling Earth Systems, 11, 2177–2213, 2019.
- Walkowiak, M. P., Walkowiak, D., and Walkowiak, J.: Exploring the paradoxical nature of cold temperature mortality in Europe, Scientific Reports, 14, 3181, 2024.
  - Wang, L., Liu, T., Hu, M., Zeng, W., Zhang, Y., Rutherford, S., Lin, H., Xiao, J., Yin, P., Liu, J., et al.: The impact of cold spells on mortality and effect modification by cold spell characteristics, Scientific reports, 6, 38 380, 2016.
- Williams, K. D., Copsey, D., Blockley, E., Bodas-Salcedo, A., Calvert, D., Comer, R., Davis, P., Graham, T., Hewitt, H., Hill, R., et al.: The

  Met Office global coupled model 3.0 and 3.1 (GC3. 0 and GC3. 1) configurations, Journal of Advances in Modeling Earth Systems, 10,
  357–380, 2018.
  - Zeka, A., Browne, S., McAvoy, H., and Goodman, P.: The association of cold weather and all-cause and cause-specific mortality in the island of Ireland between 1984 and 2007, Environmental Health, 13, 1–9, 2014.